Electronic Supplementary Material (ESI) for Physical Chemistry Chemical Physics.

Supplementary Information

Diffusion of Hydrophilic to Hydrophobic Forms of Nile Red in Aqueous $C_{12}EO_{10}$ Gels by Variable Area Fluorescence Correlation Spectroscopy

Omid Shafiee, Samantha G. Jenkins, Takashi Ito and Daniel A. Higgins**

Department of Chemistry, Kansas State University, 213 CBC Building, Manhattan, Kansas 66506-0401, USA

The synthesis of $NRSO_3^-$ and NRC_{14} dyes is described (Schemes S1 and S2). NMR and mass spectrometry data verifying that the expected products were obtained are included (Figures S1-S4). Representative two-dimensional SAXS scattering data from $C_{12}EO_{10}$ gels are also shown (Figure S5), as are fluorescence spectroscopy data for NR, $NRSO_3^-$, and NRC_{14} in a series of solvent mixtures (Figure S6) and within $C_{12}EO_{10}$ gels (Figure S7). The procedure used to determine the size of the confocal detection region (observation area) for the series of pinholes employed is described and representative data using rhodamine B as the calibration standard are provided (Figure S8). The statistical method used to verify that all three dyes exhibit free Fickian diffusion over the diffraction-limited distances probed in the $C_{12}EO_{10}$ gels is described. Results from this analysis are given in Tables S1-S3. Representative diffusion law plots for NR, $NRSO_3^-$, and NRC_{14} in ethanol solution are also included (Figure S9).

Synthesis and Characterization of Nile Red Derivatives

Characterization Methods. ^{1}H- and ^{13}C-NMR spectra were measured on a Bruker Avance NEO spectrometer (400 MHz for ^{1}H), and chemical shifts were reported in δ values in ppm downfield of tetramethylsilane. Exact MS data were measured at the Mass Spectroscopy Laboratory, University of Kansas. Fluorescence spectra were recorded on a Jobin Yvon ISA-Spex FluoroMax-2 spectrofluorometer.

Synthesis of 9-Diethylamino-2-sulfonatopropyl-5H-benzo[a]phenoxazin-5-one, potassium salt ($NRSO_3^-$). The starting material (9-diethylamino-2-hydroxy-5H-benzo[a]phenoxazin-5-one, NROH) used in this synthesis was obtained as described previously.[1] NROH was subsequently modified as shown in Scheme S1, following procedures described in the literature.[2,3]

Scheme S1. Synthesis of $NRSO_3^-$.

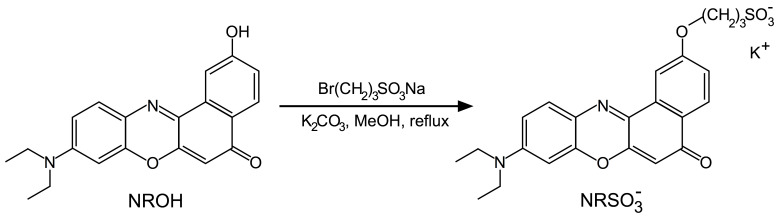

NROH (FW 354.79; 22.8 mg (0.064 mmol)) and sodium 3-bromopropanesulfonate (Alfa Aesar, FW: 225.05; 0.596 mmol) were dissolved in 2 mL anhydrous methanol, and then K_2CO_3 (Fisher, FW: 138.21; 155.59 mg (1.126 mmol)) was added. Afterwards, the mixture was refluxed under Ar with stirring for 2 days. The mixture was neutralized with an aqueous solution of acetic acid (Fisher) to achieve a 2:1 methanol:water solution. The final product was purified by reversed-phase silica gel column chromatography (C18-fully-endcapped reversed phase silica gel, Aldrich 60757; eluent: methanol:water = 2:1) to obtain a purple solid (FW: 494.23; 11.2 mg

(0.023 mmol), Yield: 36%). ^{1}H-NMR (400 MHz, CD_3OD, Figure S1): δ 8.11 (1H, d, J = 8.8 Hz), 8.05 (1H, d, J = 2.3 Hz), 7.62 (1H, d, J = 9.1 Hz), 7.22 (1H, dd, J = 8.7 Hz and 2.4 Hz), 6.85 (1H, dd, J = 9.0 and 2.2 Hz), 6.58 (1H, d, J = 2.4 Hz), 6.22 (1H, s), 4.33 (2H, t, J = 6.1 Hz), 3.55 (4H, q, J = 7.0 Hz), 3.08 (2H, t, J = 7.5 Hz), 2.37 (2H, m), 1.28 (6H, t, J = 7.1 Hz). ^{13}C-NMR (101 MHz, CD_3OD, Figure S1): δ 183.65, 161.87, 152.68, 151.54, 146.90, 138.05, 134.18, 131.09, 127.04, 124.97, 117.86, 110.44, 106.13, 103.41, 95.73, 66.79, 44.72, 24.94, 11.49. MS (Figure S2) calculated for $C_{23}H_{23}O_6N_2S^-$: 455.1277; found: M^-: 455.1271.

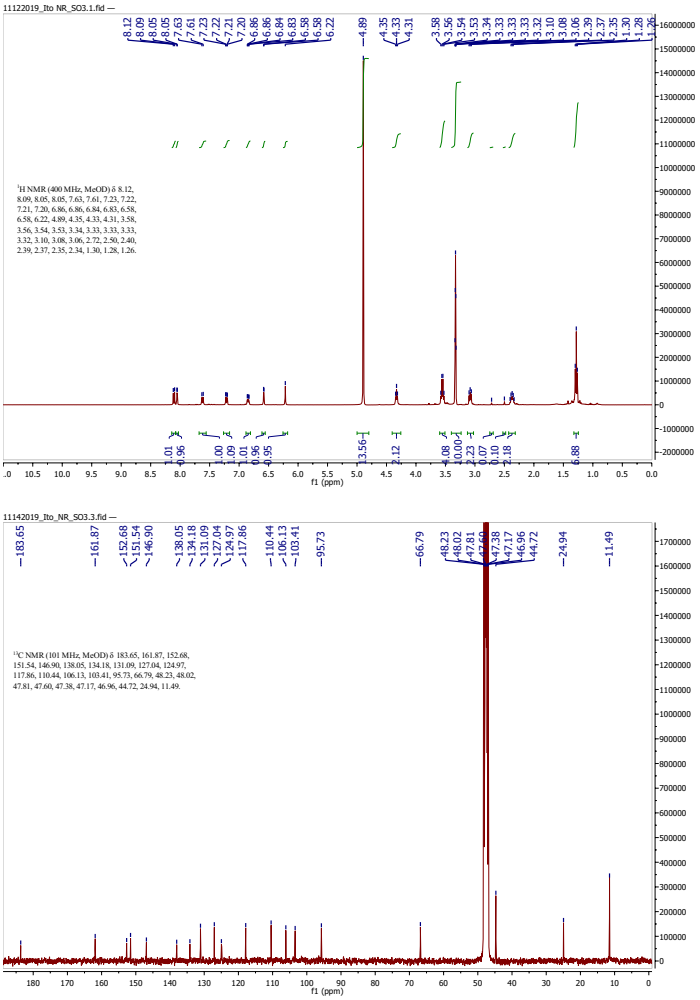

Figure S1. ^{1}H (top) and ^{13}C CD_3OD (bottom) NMR spectra for $NRSO_3^-$. A total of 19 peaks were observed in the ^{13}C NMR when 21 were expected. This difference is attributed to the overlap of peaks within the spectrum, as has been previously observed for similar derivatives of Nile red.[2] Furthermore, the -C-SO_3^- is expected to overlap with the CD_3OH peak.

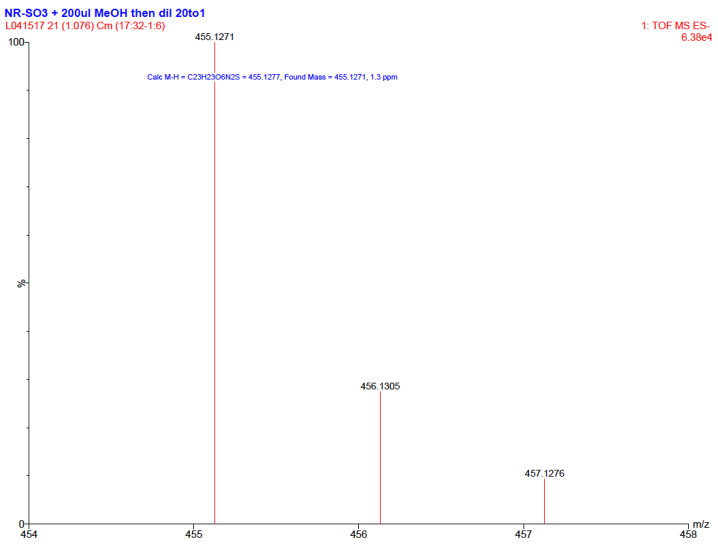

Figure S2. Mass spectrum for $NRSO_3^-$.

Synthesis of 9-Diethylamino-2-tetradecyloxy-5H-benzo[a]phenoxazin-5-one (NRC_{14}). The starting material NROH used in this synthesis was obtained as described previously.[1] NROH was subsequently modified as shown in Scheme S2, following procedures described in the literature.[2,3]

Scheme S2. Synthesis of NRC_{14}.

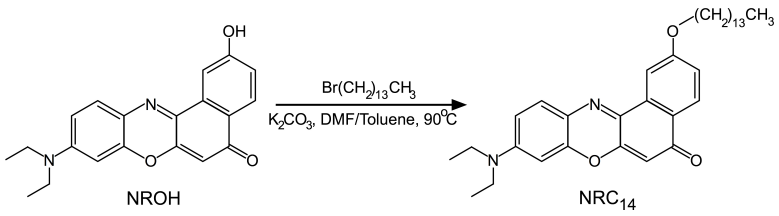

NROH (FW 354.79; 17.3 mg (0.049 mmol)) and K_2CO_3 (FW: 138.21; 35.7 mg (0.258 mmol)) was dissolved in 1.5 mL DMF with stirring at 0 °C for 30 min under Ar. Afterwards, 3 mL of toluene was added to dissolve NROH on the flask and 1-bromotetradecane (Aldrich, MW: 277.28; 23.03 mg (0.083 mmol)) was added. The mixture was then stirred in an oil bath at 90 °C under Ar overnight. The reaction mixture was next added to an aqueous solution of 0.1 M

$NaHCO_3$ and 1 M NaCl, and the crude product extracted into diethylether. The organic solution was subsequently dried with anhydrous $MgSO_4$ and the solvent was removed. The product was purified by silica gel column chromatography (petroleum ether:EtOAc = 3:1) to obtain a purple solid (FW: 530.36; 17.6 mg (0.032 mmol); Yield: 65%). ^{1}H-NMR (400 MHz, $CDCl_3$, Figure S3): δ 8.21 (1H, d, J = 8.7 Hz), 8.04 (1H, d, J = 2.6 Hz), 7.60 (1H, d, J = 9.0 Hz), 7.16 (1H, dd, J = 8.7 Hz and 2.6 Hz), 6.65 (1H, dd, J = 9.1 and 2.7 Hz), 6.45 (1H, d, J = 2.7 Hz), 6.29 (1H, s), 4.17 (2H, t, J = 6.5 Hz), 3.46 (4H, q, J = 7.1 Hz), 1.86 (2H, p, J = 6.7 Hz), 1.51 (2H, q, J = 7.4 Hz), 1.3 (26H, bs), 0.88 (3H, t, J = 6.7 Hz). ^{13}C-NMR (101 MHz, $CDCl_3$, Figure S3): δ 183.49, 162.07, 152.21, 150.84, 147.01, 140.34, 134.21, 131.19, 127.88, 125.68, 124.84, 118.44, 109.59, 106.81, 105.48, 96.48, 68.57, 59.68, 45.21, 38.30, 32.35, 32.08, 31.39, 29.84, 29.76, 29.56, 29.51, 29.39, 26.54, 26.22, 22.84, 14.27, 12.77. MS (Figure S4) calculated for $C_{34}H_{47}O_3N_2$(M+1): 531.3587; found: $(M+1)^+$: 531.3574.

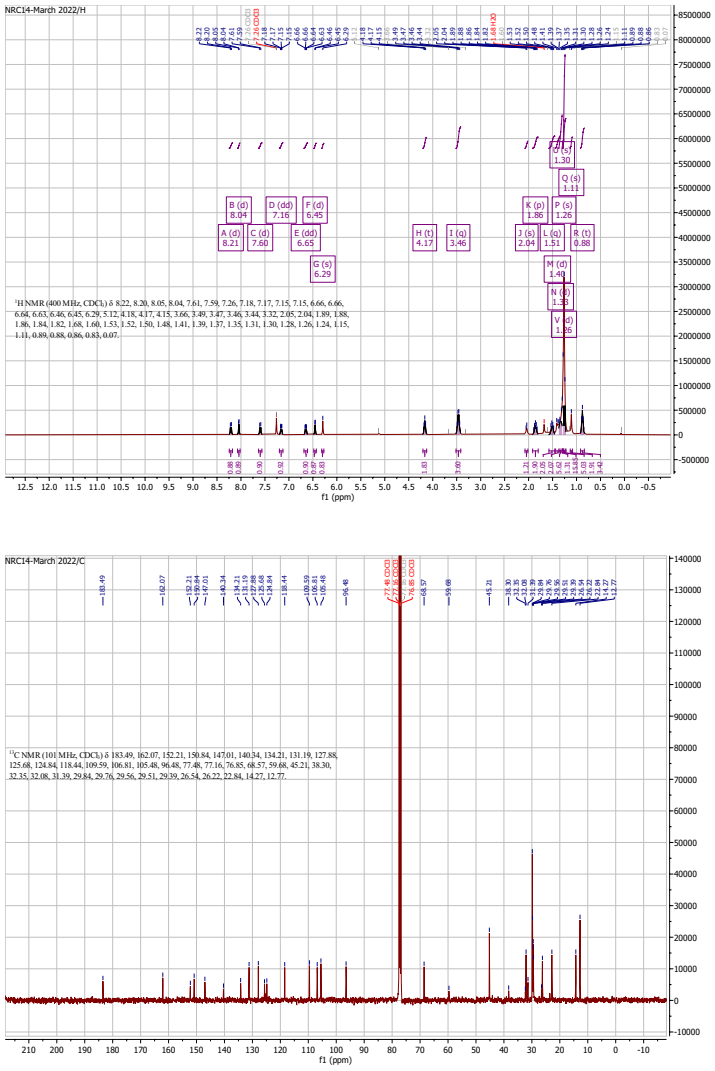

Figure S3. ^{1}H (top) and ^{13}C $CDCl_3$ (bottom) NMR spectra for NRC_{14}. A total of 33 peaks were observed in the ^{13}C NMR when 34 were expected. As in Figure S1, this difference is attributed to the overlap of peaks within the spectrum, as has been previously observed for similar derivatives of Nile red.[2]

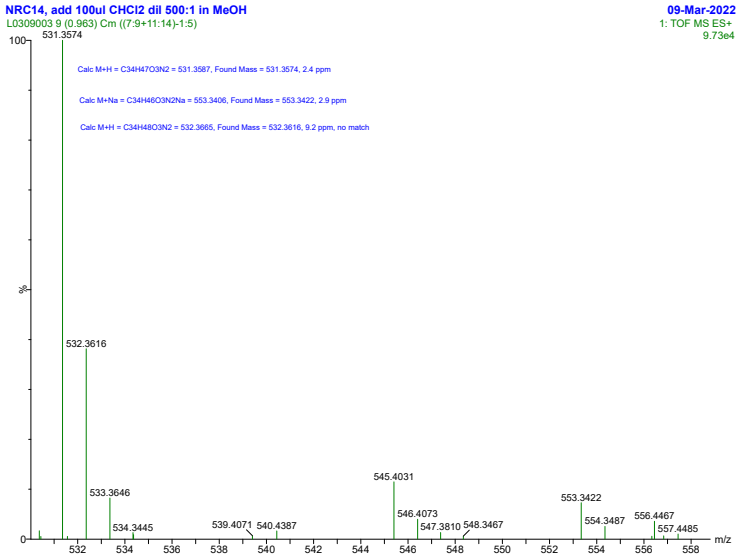

Figure S4. Mass spectrum for NRC_{14}.

$C_{12}EO_{10}$ LLC Structure and Organization

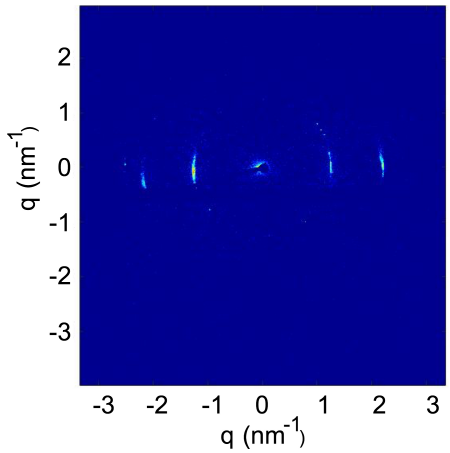

Figure S5. Two-dimensional SAXS pattern showing anisotropic scattering from a 62.5 wt% $C_{12}EO_{10}$ gel contained within a thin-walled borosilicate glass capillary. The capillary orientation corresponds to the vertical direction on the image. The results show that the cylindrical micelles are aligned with their long axes oriented along the vertical direction.

Nile Red Solvatochromism

Assessing Dye Location. The solvatochromism of the Nile red chromophore provides a means to assess the location of each of the three dyes within the $C_{12}EO_{10}$ gels. In these studies, the emission spectra of NR, $NRSO_3^-$, and NRC_{14} were first investigated in a series of solvent mixtures to confirm that their solvatochromic behaviors are similar. Representative results are shown in Figure S6. These data reveal only subtle differences in the response of the three dyes, with $NRSO_3^-$ exhibiting a small (i.e., ~ 3-4 nm) bathochromic shift in its emission, relative to the other two dyes.

Ensemble fluorescence spectra obtained from the three dyes in the $C_{12}EO_{10}$ gels were also very similar, as shown in Figure S7 for a 60:40 $C_{12}EO_{10}$ gel. The spectra exhibited no clear trends with $C_{12}EO_{10}$ concentration. Interestingly, the $NRSO_3^-$ emission spectrum is shifted to the blue of the NRC_{14} and NR spectra, but only by ~ 2 - 4 nm. These results suggest that the three dyes are found in environments of similar polarity within the gels. Unfortunately, the distance over which the Nile red chromophore responds to the polarity of its environment is unknown. It is also likely that the dye rapidly partitions between distinct environments within the gels, yielding average emission spectra.

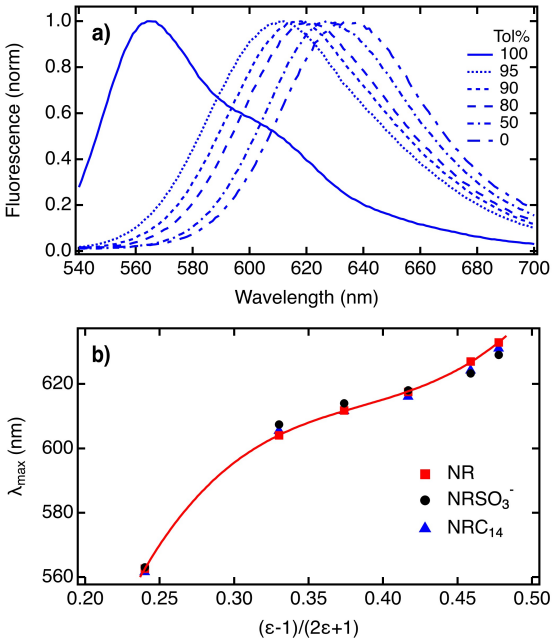

Figure S6. a) Representative fluorescence spectra obtained from NRC_{14} in mixtures of toluene and methanol. Each spectrum has been normalized to its peak value. All spectra were excited at 532 nm. **b)** Emission maximum as a function of estimated solvent Clausius-Mossotti factor for the three dyes (filled symbols).[4] The red line has been added only to better highlight the trend. These data demonstrate that NR, $NRSO_3^-$, and NRC_{14} all exhibit similar solvatochromism.

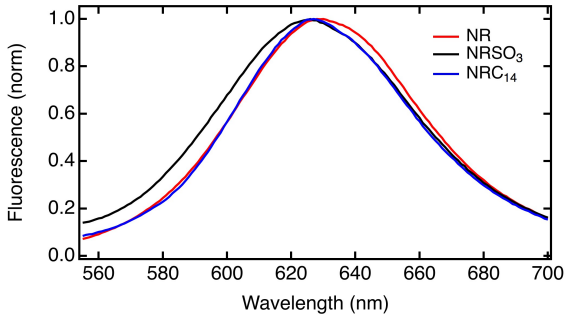

Figure S7. NR, $NRSO_3^-$, and NRC_{14} fluorescence spectra in 60:40 $C_{12}EO_{10}$ gels. The spectra were all recorded using 532 nm excitation and each has been normalized to its peak value.

Calibration of Confocal Detection Area

The confocal detection area (volume) for each pinhole size was calibrated using solutions of 5 nM RhB in ethanol. The diffusion coefficient of RhB in ethanol was determined to be 364 μm^2/s, as determined from its literature value in water.[5,6] Its diffusion time, τ_D, in ethanol was obtained by analyzing autocorrelation data (fit to Eq. 2) at each pinhole size. In this case, $\alpha = 1$ was used during fitting of the data as no diffusion anomalies are expected in bulk ethanol solution. Calibration was performed for pinholes of 50, 60, 70, 80, 90, 100, and 125 μm diameters. The calibrated radial area of the confocal detection regions was then obtained from Eq. S1:

$$\omega_r^2 = 4D\tau_D \qquad \text{(Eq. S1)}$$

The results are plotted in Figure S8, with the calibrated values of ω_r^2 given on the right ordinate.

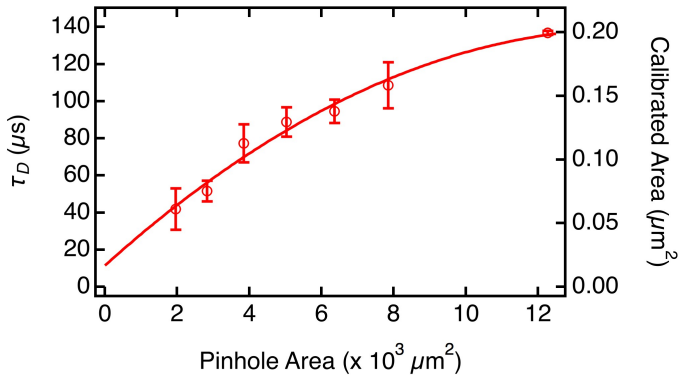

Figure S8. Mean diffusion time for Rhodamine B dye in ethanol solution as a function of geometric pinhole area. The error bars show the 95% confidence intervals from three replicate measurements. The calibrated detection area, ω_r^2, is shown on the right ordinate. The detection area was determined from $\omega_r^2 = 4D\tau_D$, with D = 364 μm^2/s as estimated from its literature value in water.[5,6] The solid line has been appended to better show the trend in the data. The pinholes employed in calibration of the observation area were of 50, 60, 70, 80, 90, 100, and 125 μm diameters.

Variable Area FCS Measurements and Diffusion Law Analysis

Statistical Assessment of Diffusion Law Analysis Results. The analysis of va-FCS data involves determination of whether plots of the measured diffusion time, τ_D, vs. detection area, ω_r^2, produce a non-zero intercept when a line produced by linear regression of the data is extrapolated to zero area.[7,8] While such an assessment may be qualitatively reasonable, a quantitative statistical analysis of the intercept deviation from zero is challenging. First, the diffraction-limited nature of the method precludes collection of data from detection areas near zero. Statisticians caution against extrapolating to zero under such circumstances.[9] Furthermore, the usual method[10] for assessing the error on the intercept under these conditions does not produce good estimates its value, precluding its use in the usual hypothesis tests.

Here, a simple variant of the above method has been implemented as a means to achieve a valid statistical test of diffusion law analysis results. In this method, the observation area values are simply shifted so that zero corresponds to their mean value, $X_0 = \overline{\omega_r^2}$. The data are then fit by linear regression to a line, $Y = m(X - X_0) + b$. The intercept, b, in this case, falls within the range of measured values and the usual method[10] of estimating its error remains valid. The statistical test employed is the Student's T-test and involves comparing b to the product $m \times \overline{\omega_r^2}$ using the null hypothesis that b = $m \times \overline{\omega_r^2}$. The usual standard errors on the values of m (SE_m) and b (SE_b) are employed, along with that of $\overline{\omega_r^2}$ (SE_{X_0}). Then, the standard error on the product, SE_p, is calculated as:

$$SE_p = \sqrt{\left(\overline{\omega_r^2}\right)^2 SE_m^2 + m^2 SE_{X_0}^2} \qquad \text{(Eq. S2)}$$

The calculated t-statistic is obtained from:

$$t_{calc} = \frac{\left|b - m\overline{\omega_r^2}\right|}{\sqrt{SE_b^2 + SE_p^2}} \qquad \text{(Eq. S3)}$$

The null hypothesis is rejected if $t_{calc} > t_{table}$, where t_{table} is the Student t value obtained at the 95% confidence level, with the specified degrees of freedom. Tables S1-S3 summarize the results from NR, $NRSO_3^-$, and NRC_{14} in the $C_{12}EO_{10}$ gels and glycerin-ethanol mixtures. Data in the tables were compiled from three replicate measurements on each type of sample.

Table S1. Statistical analysis of NR data in $C_{12}EO_{10}$ gels as a function of gel composition (surfactant:water wt%) and in homogeneous 75:25 wt% glycerin-ethanol solution.

NR[a]	**55:45**	**60:40**	**65:35**	**70:30**	**Gly:EtOH**
m ($x10^3$)	38.0	37.2	39.0	30.1	47.2
$\mathbf{SE_m}$ ($x10^3$)	3.7	4.9	8.6	2.5	3.9
b ($x10^3$)	5.70	6.22	6.13	4.96	8.14
$\mathbf{SE_b}$ ($x10^3$)	0.11	0.15	0.26	0.07	0.12
$\boldsymbol{m\overline{\omega_r^2}}$ ($x10^3$)	5.61	5.48	5.76	4.45	6.96
$\mathbf{t_{calc}}$[b]	0.121	0.789	0.252	0.876	1.273
Null Hyp.	accept	accept	accept	accept	accept

[a] In all cases $\overline{\omega_r^2} = 0.148$ and $SE_{X_0} = 0.015$.
[b] SE_p and t_{calc} are obtained from Eq. S2 and Eq. S3. The value $t_{table} = 2.262$ (95% confidence, 9 degrees of freedom).

Table S2. Statistical analysis of $NRSO_3^-$ data in $C_{12}EO_{10}$ gels as a function of gel composition (surfactant:water wt%) and in homogeneous 75:25 wt% glycerin-ethanol solution.

$NRSO_3^-$ [a]	**55:45**	**60:40**	**65:35**	**70:30**	**Gly:EtOH**
m ($x10^3$)	27.4	29.9	42.7	44.7	60.7
SE_m ($x10^3$)	7.1	5.2	11.3	6.1	18.2
b ($x10^3$)	5.10	5.65	7.21	7.94	11.4
SE_b ($x10^3$)	0.21	0.15	0.34	0.18	0.54
$m\overline{\omega_r^2}$ ($x10^3$)	4.05	4.41	6.30	6.60	8.96
t_{calc} [b]	0.925	1.384	0.500	1.187	0.831
Null Hyp.	accept	accept	accept	accept	accept

[a] In all cases $\overline{\omega_r^2}$ = 0.148 and SE_{X_0} = 0.015.
[b] SE_p and t_{calc} are obtained from Eq. S2 and Eq. S3. The value t_{table} = 2.262 (95% confidence, 9 degrees of freedom).

Table S3. Statistical analysis of NRC_{14} data in $C_{12}EO_{10}$ gels as a function of gel composition (surfactant:water wt%). Glycerin-ethanol data were not collected due to limited solubility of the dye.

NRC_{14} [a]	**55:45**	**60:40**	**65:35**	**70:30**	**Gly:EtOH**
m ($x10^3$)	52.9	41.3	54.1	50.9	NA
SE_m ($x10^3$)	5.5	7.8	4.0	15.9	NA
b ($x10^3$)	11.4	9.26	10.5	11.4	NA
SE_b ($x10^3$)	0.21	0.30	0.15	0.61	NA
$m\overline{\omega_r^2}$ ($x10^3$)	10.1	7.88	10.3	9.71	NA
t_{calc} [b]	0.883	0.802	0.163	0.533	NA
Null Hyp.	accept	accept	accept	accept	NA

[a] In all cases $\overline{\omega_r^2}$ = 0.191 and SE_{X_0} = 0.019.
[b] SE_p and t_{calc} are obtained from Eq. S2 and Eq. S3. The value t_{table} = 2.262 (95% confidence, 9 degrees of freedom).

Variable Area FCS Studies of Dye Diffusion in Ethanol. va-FCS experiments were also performed on NR, $NRSO_3^-$, and NRC_{14} in bulk ethanol solution. These experiments provided controls that support the interpretations of va-FCS data obtained from the $C_{12}EO_{10}$ gels. Figure S9 plot the results obtained. The data are all statistically consistent with free Fickian diffusion in bulk ethanol solution, as expected. The data yield D_{Law} values of 470 ± 10 $\mu m^2/s$, 310 ± 20 $\mu m^2/s$, and 280 ± 20 $\mu m^2/s$ for NR, NRC_{14}, and NRSO3$^-$, respectively. The smaller D_{Law} value obtained from NRC_{14} was expected, based on the increase in molecular size. The smaller D_{Law} obtained from $NRSO_3^-$ may result from a difference in solvation and/or the presence of the potassium counter ion.

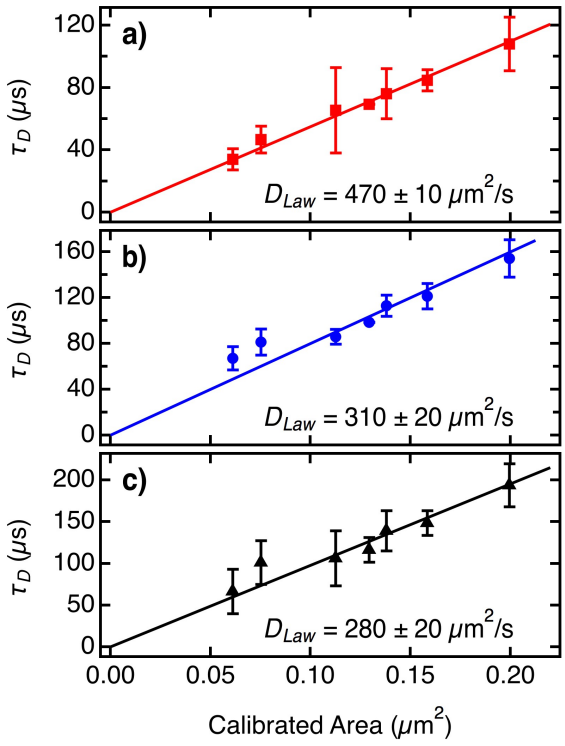

Figure S9. **a)** NR (red squares), **b)** NRC_{14} (blue circles) and **c)** $NRSO_3^-$ (black triangles) diffusion times as a function of detection area in ethanol solution. The solid lines depict fits of the data to Eq. 3 with $\tau_0 = 0$. Mean D_{Law} values obtained from three replicate measurements in each case are shown. The pinholes employed were of 50, 60, 70, 80, 90, 100, and 125 μm diameters. Error bars depict 95% confidence intervals on the autocorrelation fitting parameters.

References

(1) Martin-Brown, S. A.; Fu, Y.; Saroja, G.; Collinson, M. M.; Higgins, D. A. Single-Molecule Studies of Diffusion by Oligomer-Bound Dyes in Organically Modified Sol-Gel-Derived Silicate Films. *Anal. Chem.* **2005**, *77*, 486-494.

(2) Briggs, M. S. J.; Bruce, I.; Miller, J. N.; Moody, C. J.; Simmonds, A. C.; Swann, E. Synthesis of Functionalised Fluorescent Dyes and Their Coupling to Amines and Amino Acids. *J. Chem. Soc. Perkin Trans. 1* **1997**, 1051-1058.

(3) Kucherak, O. A.; Oncul, S.; Darwich, Z.; Yushchenko, D. A.; Arntz, Y.; Didier, P.; Mély, Y.; Klymchenko, A. S. Switchable Nile Red-Based Probe for Cholesterol and Lipid Order at the Outer Leaflet of Biomembranes. *J. Am. Chem. Soc.* **2010**, *132*, 4907-4916.

(4) Giri, D.; Hanks, C. N.; Collinson, M. M.; Higgins, D. A. Single-Molecule Spectroscopic Imaging Studies of Polarity Gradients Prepared by Infusion-Withdrawal Dip-Coating. *J. Phys. Chem. C* **2014**, *118*, 6423-6432.

(5) Culbertson, M. J.; Williams, J. T. B.; Cheng, W. W. L.; Stults, D. A.; Wiebracht, E. R.; Kasianowicz, J. J.; Burden, D. L. Numerical Fluorescence Correlation Spectroscopy for the Analysis of Molecular Dynamics under Nonstandard Conditions. *Anal. Chem.* **2007**, *79*, 4031-4039.

(6) Gendron, P.-O.; Avaltroni, F.; Wilkinson, K. J. Diffusion Coefficients of Several Rhodamine Derivatives as Determined by Pulsed Field Gradient-Nuclear Magnetic Resonance and Fluorescence Correlation Spectroscopy. *J. Fluoresc.* **2008**, *18*, 1093-1101.

(7) Wawrezinieck, L.; Rigneault, H.; Marguet, D.; Lenne, P.-F. Fluorescence Correlation Spectroscopy Diffusion Laws to Probe the Submicron Cell Membrane Organization. *Biophys. J.* **2005**, *89*, 4029-4042.

(8) Veerapathiran, S.; Wohland, T. The Imaging FCS Diffusion Law in the Presence of Multiple Diffusive Modes. *Methods* **2018**, *140-141*, 140-150.

(9) Milliken, G. A.; Johnson, D. E.: *Analysis of Messy Data, Volume III: Analysis of Covariance*; Chapman & Hall/CRC Press: Boca Raton, FL, 2002.

(10) Harris, D. C.; Lucy, C. A.: *Quantitative Chemical Analysis*; W. H. Freeman: Austin, TX, 2020.